DOI: https://doi.org/10.14311/TPFM.2025.038

EFFECT OF BLADE VIBRATIONS ON TURBULENCE STRUCTURE

V. Yanovych[1], V. Tsymbalyuk[1], D. Duda[1], V. Uruba[1, 2], M. Klimko[1]

[1] Department of Power System Engineering, Faculty of Mechanical Engineering, University of West Bohemia, Univerzitní 8, Pilsen 301 00, Czech Republic

[2] Czech Academy of Sciences, Institute of Thermomechanics, Dolejškova 5, Prague 182 00, Czech Republic

Abstract

This study explores the influence of blade vibrations on the turbulent flow structure within a low-pressure turbine blade cascade. Hot-wire anemometry was applied to compare flow patterns around a stationary blade and those during bending and torsional vibrations. The experiments were conducted at a flow velocity corresponding to a chord-based Reynolds number of $Re_c = 2.3\times10^5$ and an excitation frequency of 73 Hz. The results demonstrate that, unlike torsion, bending vibrations reduce the streamwise velocity deficit by 5% downstream of the blade compared to its stationary state. Furthermore, bending vibrations enhance the formation of large vortices, resulting in a fivefold increase in the integral length scale. In contrast, the Kolmogorov microscale remains unchanged under all experimental scenarios, reaching its minimum in the wake region and maximum in the inter-blade space.

Keywords: blade vibrations, hot-wire, scales of turbulence, energy dissipation rate

1 Introduction

Blade aeroelastic instability, commonly known as "blade flutter," presents a significant challenge in turbomachinery. Over the past few decades, extensive research has focused on understanding flutter instability in turbine blade cascades. However, the substantial financial and operational limitations associated with experimental methods led most studies to investigate this phenomenon using numerical fluid dynamics simulations. These studies show that blade aeroelastic instability induces significant modifications in the turbulent flow structure, leading to the formation of multiscale coherent structures that subsequently influence the overall aerodynamic behavior and efficiency of turbomachinery [1-5].

However, despite advancements in numerical methodologies, the accurate determination of turbulent structures and the comprehensive analysis of underlying physical mechanisms, such as energy dissipation rates, remain significant challenges. A primary barrier in this field is the lack of reliable experimental data on flow-blade interactions, which is crucial for validating and refining numerical models. Addressing this data gap is essential for improving our understanding and preventing aeroelastic instability in turbine blades. Therefore, this study emphasizes the experimental analysis of turbulent structure in the wake of a vibrating blade.

2 Experimental setup

The experiments were performed in a blowdown wind tunnel developed by the Department of Power System Engineering at the University of West Bohemia [6, 7]. Figure 1 a) provides an overview of the test section's design. The blade cascade consisted of eight blades, four of which were movable. The blades represented scaled-down models of the tip profile of the last-stage blade of a steam turbine rotor, with a chord length of c = 50 mm, a span of h = 79.5 mm, and a maximum thickness of b = 2.2 mm. The blade incidence angle was θ = -2°, with a pitch of t = 46 mm and a stagger angle of 72°. The dimensions of the inlet channel were 80 mm in height and 59.2 mm in width. Figure 2 b) illustrates the geometry of the vibrating blade cascade. The study was carried out at a chord-based Reynolds number of $Re_c = 2.3\times10^5$, calculated based on the inflow velocity $U = 70\ \mathrm{m\cdot s^{-1}}$. It primarily focused on examining turbulence structure under stationary state, as well as during bending and torsional vibrations of blade 2. The blade's vibration frequency was f = 73 Hz, with oscillation amplitudes of 0.5° in the torsional mode and 0.7 mm in the bending mode. Measurements were conducted at a cross-section 3 mm downstream of the trailing edge at mid-blade height. The measurement region encompassed two pitch periods, covering blades 2 and 3, with a point spacing of 1.5 mm.

The experiments employed a hot-wire anemometer equipped with a miniature 55P63 X-wire probe. Hot-wire signals in all experiments were sampled at a frequency of 250 kHz and signal filtering was applied. The high-pass and low-pass filter cut-off frequencies were set at 10 Hz and 30 kHz, respectively. Each single-point measurement lasted 10 s. Accordingly to methodologies [8-11], the uncertainty of the conversion process of a probe's electrical signal into velocity samples was about ±0.5%.

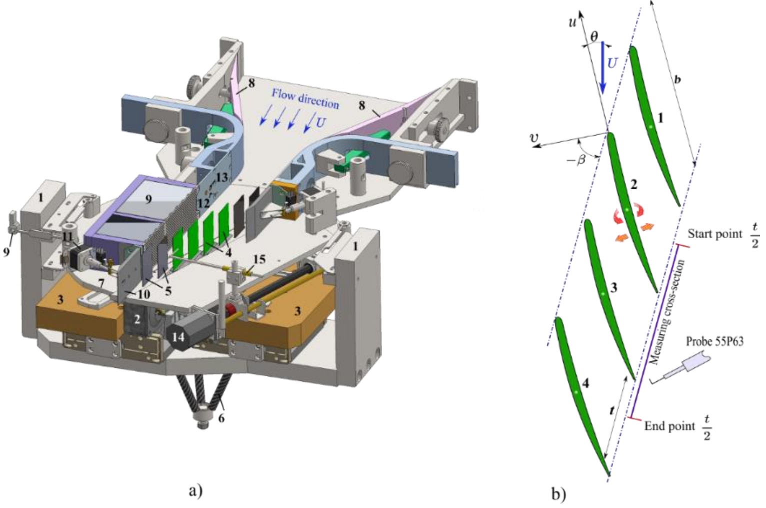

Figure 1: a) Configuration of the test section. The components are designated as follows: 1 – frame body; 2- electromagnetic shakers; 3 - damper mass of electromagnetic shaker; 4 – flexibly mounted blade (marked in green); 5 - rigid blade (marked in gray); 6 - frame spring; 7 - rotating disk; 8 – adjustable inlet nozzle walls; 9 – muffler; 10 - directional flaps; 11 - stepper motor of directional flap; 12- flush-mounted static port; 13 - Pitot probe; 14 - traversing system; 15 – probe support. b) Geometry of the turbine blade cascade. The blue arrow indicates the flow direction, while the blue line represents the hot-wire measurement cross-section.

1 Result and discussion

The initial assessment focused on evaluating the impact of vibrations on the wake topology downstream of the blade cascade. Figure 2 presents a comparative analysis of the normalized streamwise and spanwise velocity distributions across different experimental conditions. For improved visualization, the measurement positions of the collected data were normalized by the pitch. As a result, the trailing edges of blades 2 and 3 were positioned at $z{\cdot}t^{-1} = 0$ and $z{\cdot}t^{-1} = 1$, respectively.

The findings reveal a pronounced impact of the bending mode on wake topology, resulting in a 5% reduction in the streamwise velocity deficit relative to the stationary and torsional modes. Furthermore, the velocity profiles acquired under varying experimental conditions consistently indicate that the wake core is displaced toward the suction side. This effect is primarily due to the boundary layer expansion on the suction side, driven by the blade's asymmetric geometry and angle of attack [12-14].

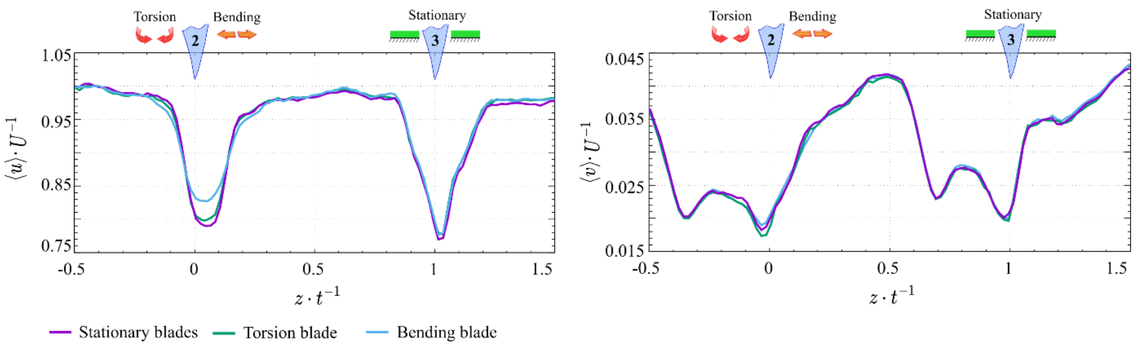

Figure 2: Normalized streamwise u and spanwise υ velocity distributions across different experimental conditions.

The interaction between the vibrating blade and the surrounding flow naturally leads to turbulence. Therefore, the following research stage analyzed the characteristics of turbulent kinetic energy and turbulence intensity across different blade modes. Each parameter was computed based on the streamwise u and spanwise v velocity components:

$$TKE = 0.5\,(\langle u' \rangle^2 + \langle v' \rangle^2) \tag{1}$$

and

$$TI = \sqrt{\frac{\langle u' \rangle^2 + \langle v' \rangle^2}{\langle u \rangle^2 + \langle v \rangle^2}} \tag{2}$$

where $\langle u' \rangle$ and $\langle v' \rangle$ represent the time-averaged velocity fluctuations, while $\langle u \rangle$ and $\langle v \rangle$ denote the mean velocities in the streamwise and spanwise directions, respectively.

Figure 3 illustrates the normalized distribution of turbulent kinetic energy and turbulence intensity across different experimental conditions. The data obtained indicate that the bending mode leads to a 1.52-fold increase in turbulent kinetic energy and a 1.25-fold increase in turbulence intensity compared to the stationary and torsional modes. This effect is attributed to the unique vortex formation mechanism induced by blade motion. In stationary and torsional modes, flow separation occurs later, followed by the rolling up and recirculation of the shear layer on the suction side, generating smaller vortex structures over time. In contrast, the bending mode accelerates flow separation, promoting the formation of larger and more dynamic vortices. These structures exhibit higher turbulent kinetic energy, intensifying flow instability relative to the stationary and torsional modes.

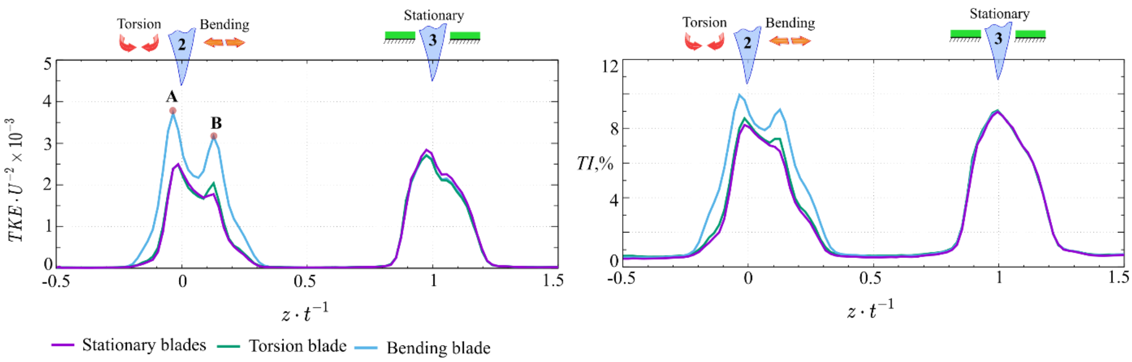

Figure 3: Normalized turbulent kinetic energy *TKE* and turbulence intensity *TI* distributions across different experimental conditions.

The power spectral density method was employed to analyze the distribution of energy flux intensity between various scale turbulence structures. For this analysis, measurement points A and B were selected (see Fig. 3), corresponding to the maximum turbulent kinetic energy locations on the blade's pressure and suction sides.

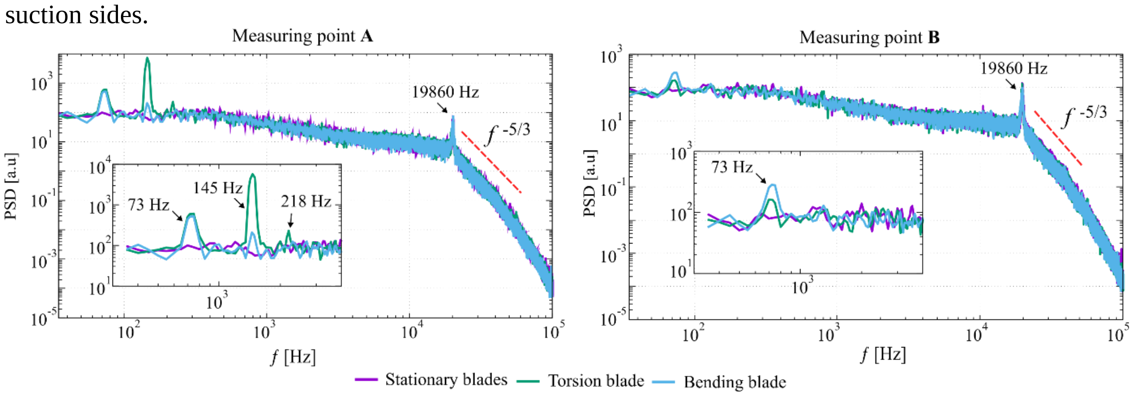

Figure 4: Power spectral density at measurement points A and B across different experimental conditions. The small panel highlights the location of the excitation frequency-related harmonics.

Figure 4 presents the graphical interpretation of power spectral densities of streamwise velocity fluctuations across different experimental conditions**.** The resulting distributions show localized power surges marked by distinct spectral peaks. From a turbulence perspective, significant spikes in signal power generally correspond to the presence of large-scale vortex structures. However, the formation mechanisms of these structures vary. Peaks below 300 Hz are predominantly linked to blade vibrations, indicating active vortex breakdown propagation within the wake region. Specifically, the 73 Hz, 145 Hz, and 218 Hz peaks correspond to the first, second, and third harmonics of the blade's excitation frequency. In contrast, the spectral burst observed at 19860 Hz is associated with the vortex shedding frequency. Moreover, the obtained spectral distributions clearly exhibit a characteristic slope of the curve $f^{-5/3}$. According to Kolmogorov's theory [15], this slope suggests an isotropic, homogeneous nature of the turbulent flow.

The follow-up stage of the study focused on evaluating the impact of blade vibration on the turbulent flow structure. For this purpose, a well-established methodology, as previously documented in references [16-19], was implemented. The initial step in analyzing turbulence structures involves evaluating the integral length scale, which defines the characteristic size of the most energetic and dominant vortices in a turbulent flow. To determine this scale, an autocorrelation function is typically employed, where its intersection with the spatial axis defines the characteristic scale of the largest vortices [20-22]. However, in the presence of blade vibration, the autocorrelation function curve exhibits pronounced periodic behavior, which significantly complicates the precise identification of the correct intersection point with the spatial axis. Therefore, the Roach method [23], based on energy spectrum estimation, was applied to determine the integral length scale L_R.

$$L_R = \frac{E(f)_{500} \cdot \langle u \rangle}{4\sigma_u^2} \tag{3}$$

where $E(f)_{500}$ represents the average value calculated from the first 500 data points within the energy spectrum distribution, and σ_u is standard deviation of streamwise velocity component u.

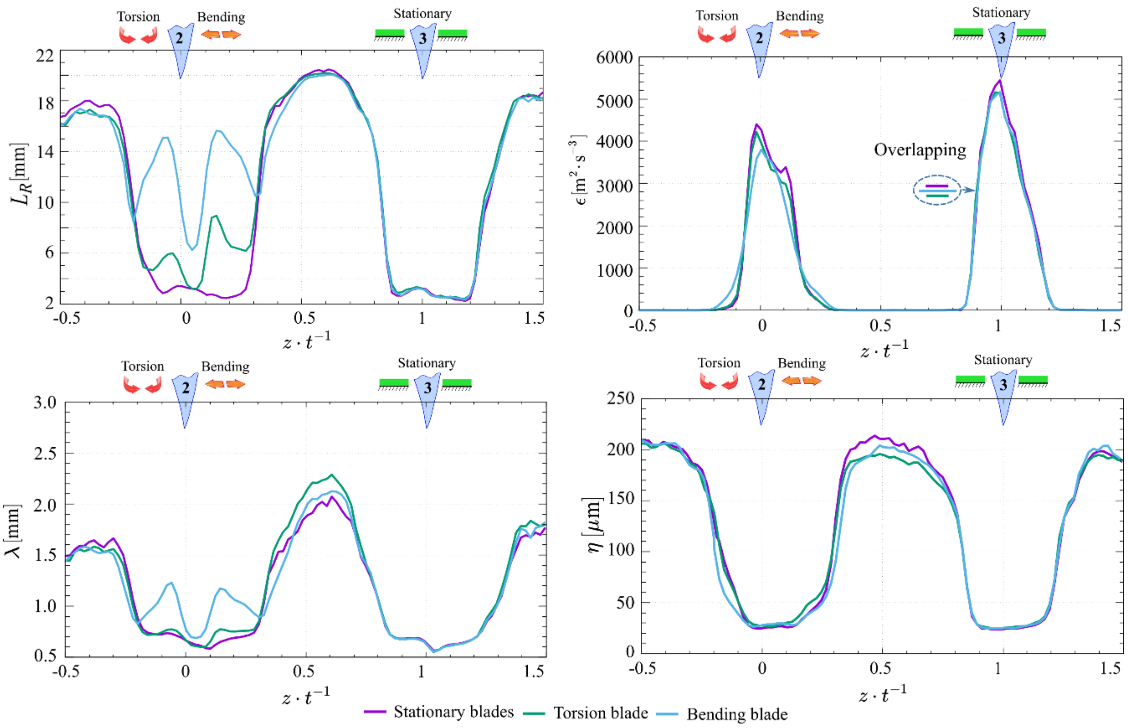

Figure 5: Structure of turbulence for different blade modes, where L_R represents integral length scales calculated based on the Roch approach, λ denotes Taylor microscales, η corresponds to Kolmogorov microscales, and ϵ indicates the energy dissipation rate.

Figure 5 shows the distribution of the integral length scale across different experimental scenarios. The data indicate fivefold increases in the size of the largest vortices in the bending mode and twofold in the torsion mode compared to the stationary mode. This feature is due to the distinct characteristics of vortex formation under various blade modes. This feature is directly linked to the intensity and nature of the flow disturbances introduced by each blade motion type. In the bending mode, large perpendicular oscillations enhance vortex shedding and energy transfer, leading to significantly larger coherent structures. In contrast, the torsion mode, characterized by angular oscillations, induces periodic variations in flow separation, increasing vortex size to a lesser extent. The stationary mode serves as a baseline, where vortex formation is governed by natural boundary layer separation.

The energy dissipation rate is one of the fundamental parameters in the evolution of turbulent flow [24, 25]. The Kolmogorov approach was applied to estimate this parameter based on scaling the second-order longitudinal structure function within the inertial range.

$$\epsilon = \frac{(D_{LL}(\rho)/C)^{\frac{3}{2}}}{\rho} \tag{4}$$

where C is a empirical constant C ~2, while $D_{LL}(\rho)$ is streamwise second-order structure function.

$$D_{LL}(\rho) = \langle [u(x+\rho) - u(x)]^2 \rangle \tag{5}$$

As shown in Fig. 5, the maximum value of 4200 $m^2 \cdot s^{-3}$ occurs in the stationary mode, while the minimum value of 3400 $m^2 \cdot s^{-3}$ is observed in the bending mode. Additionally, higher values of dissipation rate are consistently observed on the pressure side, where stronger shear stresses and turbulence generation occur due to higher pressure gradients.

Once the dissipation rate is known, Taylor λ and Kolmogorov η microscales can be estimated from classical relations:

$$\eta = \left(\frac{\nu^3}{\epsilon}\right)^{1/4} \tag{6}$$

and

$$\lambda = \sigma_u \sqrt{15 \frac{\nu}{\epsilon}} \tag{7}$$

where ν represents the kinematic viscosity

The results obtained illustrate the growth of the Taylor microscale in the wake region under the bending mode. Specifically, the value of λ nearly twofold compared to the stationary and torsion modes. Meanwhile, the Kolmogorov microscale remains unchanged during blade vibration. In the wake region, the smallest vortices with a size of η = 30 µm are observed, while in the inter-blade region, their size increases to η = 200 µm.

4 Conclusion

The study investigated the impact of blade vibrations on the wake topology and turbulence structure downstream of a low-pressure turbine blade cascade. The experiments employed hot-wire anemometry using an X-wire probe (55P63) at a flow velocity corresponding to a chord-based Reynolds number of $Re_c = 2.3\times10^5$, where c = 50 mm. A comparative analysis of flow patterns between a stationary blade and those during its bending and torsion vibrations was conducted. The excitation frequency of the vibration was f =73 Hz, with oscillation amplitudes of 0.5° for torsion and 0.7 mm for bending mode. The experimental data were used to derive graphical distributions of flow velocity, turbulent kinetic energy, and turbulence intensity in both streamwise and spanwise directions. The results highlight the substantial influence of the bending mode on wake topology. Compared to stationary and torsional modes, the bending mode reduces the streamwise velocity deficit by 5%. Additionally, in the wake region, the bending mode enhances turbulent kinetic energy and turbulence intensity, increasing them by factors of 1.52 and 1.25, respectively. Furthermore, the turbulence structure was examined across different experimental scenarios. Using the Roach method, the integral length scale revealed that the largest vortices expanded fivefold in the bending mode and twofold in the torsion mode compared to the stationary case. In the wake region, the Taylor microscale doubled in the bending mode, while the Kolmogorov microscale remained largely unchanged. Additionally, bending vibrations resulted in a 20% reduction in the energy dissipation rate.

References

[1] Fürst, J., Lasota, M., Lepicovsky, J., Musil, J., Pech, J., Šidlof, P., Šimurda, D.: Effects of a single blade incidence angle offset on adjacent blades in a linear cascade. *Processes*, vol. 9, (2021).

[2] Camp, T.R., Shin, H.W.: Turbulence intensity and length scale measurements in multistage compressors, *ASME. J. Turbomach*, 117(1), (1995), pp. 38–46.

[3] Rahmati, M., He, L., Wang, D., Li, Y., Wells, R., Krishnababu, S.: Non-linear time and frequency domain methods for multi-row aeromechanical analysis. *Proceedings of ASME Turbo Expo 2012*, pp. 1473-1485, (2012).

[4] Rahmati, M., He, L., Wells, R.: Interface treatment for harmonic solution in multi-row aeromechanic analysis. *Proceedings of ASME Turbo Expo 2010*, pp. 1253-1261, (2010).

[5] Oro, J., Argüelles Díaz, K., Santolaria, C., Marigorta, E.: On the structure of turbulence in a low-speed axial fan with inlet guide vanes. *Experimental Thermal and Fluid Science*, vol. 32, (2007), pp. 316-331.

[6] Eret, P., Tsymbalyuk, V.: Experimental subsonic flutter of a linear turbine blade cascade with various mode shapes and chordwise torsion axis locations. *Journal of Turbomachinery*, vol. 145, (2022), pp. 1-12.

[7] Yanovych, V., Duda, D., Horáček, V., Uruba, V.: Research of wind tunnel parameters by means of cross-section analysis of air flow profiles. *AIP Conference Proceedings*, vol. 2189, (2019), art. no. 020024.

[8] Jonás, P.: Rotary slanted single wire CTA – a useful tool for 3D flow investigations. *EPJ Web of Conferences*, vol. 45, (2013), 01047.

[9] King, L.V., Barnes, H.T.: On the convection of heat from small cylinders in a stream of fluid: Determination of the convection constants of small platinum wires, with applications to hot-wire anemometry. *Proceedings of the Royal Society of London. Series A, Containing Papers of a Mathematical and Physical Character*, vol. 90, (1914), pp. 563-570.

[10] Bruun, H.: Interpretation of a hot wire signal using a universal calibration law. *Journal of Physics E: Scientific Instruments*, vol. 4, (1971), pp. 225-231.

[11] Bruun, H.: Hot wire data corrections in low and in high turbulence intensity flows. *Journal of Physics E: Scientific Instruments*, vol. 5, (1972), pp. 812-818.

[12] Duda, D., Uruba, V., Yanovych, V.: Wake width: Discussion of several methods to estimate it using measured experimental data. *Energies*, vol. 14, no. 15, (2021), art. no. 4712.

[13] Yanovych, V., Duda, D., Uruba, V., Antoš, P.: Anisotropy of turbulent flow behind an asymmetric airfoil. *SN Applied Sciences*, vol. 3, no. 12, (2021), art. no. 885.

[14] Duda D., Yanovych V., Tsymbalyuk V., Uruba V. Effect of Manufacturing Inaccuracies on the Wake Past Asymmetric Airfoil by PIV (2022) Energies, 15 (3), art. no. 1227

[15] Kolmogorov, A.: The local structure of turbulence in incompressible viscous fluid for very large Reynolds numbers. *Doklady Akademii Nauk SSSR*, vol. 30, (1941), pp. 301-305. (in Russian); English translation: *Proceedings of the Royal Society A*, vol. 434, (1991), pp. 9-13.

[16] Davidson, P.: *Turbulence: An Introduction for Scientists and Engineers*. Oxford University Press, (2015).

[17] Davies, P.: Structure of turbulence. *Journal of Sound and Vibration*, vol. 28, (1973), pp. 513-526.

[18] Batchelor, G.K.: *The Theory of Homogeneous Turbulence*. Cambridge University Press, New York, USA, (1982).

[19] Bauinger, S., et. al: On turbulence measurements and analyses in a two-stage two-spool turbine rig. *Journal of Turbomachinery*, vol. 137, (2017), 071008.

[20] Bourgoin, M. et al.: Investigation of the small-scale statistics of turbulence in the Modane S1MA wind tunnel. *CEAS Aeronautical Journal*, vol. 9, (2018), pp. 269-281.

[21] Yanovych, V., Duda, D., Uruba, V.: Structure of turbulent flow behind a square cylinder with an angle of incidence. *European Journal of Mechanics, B/Fluids*, vol. 85, (2021), pp. 110-123.

[22] Yanovych, V., Duda, D., Uruba, V., Tomášková, T.: Hot-wire investigation of turbulence topology behind blades at different shape qualities. *Processes*, vol. 10, no. 3, (2022), art. no. 522.

[23] Roach, P.E.: The generation of nearly isotropic turbulence by means of grids. *International Journal of Heat and Fluid Flow*, vol. 8, no. 2, (1987), pp. 82-92.

[24] Kolmogorov, A.: Dissipation of energy in locally isotropic turbulence. *Proceedings of the Royal Society of London. Series A. Mathematical and Physical Sciences*, vol. 1890, (1991), pp. 15-17.

[25] Wang, G., Yang, F., Wu, K., Ma, Y., Peng, C., Liu, T., Wang, L.P.: Estimation of the dissipation rate of turbulent kinetic energy: A review. *Chemical Engineering Science*, vol. 229, (2021), 116133.